Nonhydrodynamic modes and *a priori* construction of shallow water lattice Boltzmann equations

Paul J. Dellar*
Department of Applied Mathematics and Theoretical Physics, University of Cambridge, Silver Street, Cambridge CB3 9EW, United Kingdom
(Received 13 October 2001; published 15 February 2002)

Lattice Boltzmann equations for the isothermal Navier-Stokes equations have been constructed systematically using a truncated moment expansion of the equilibrium distribution function from continuum kinetic theory. Applied to the shallow water equations, with its different equation of state, the same approach yields discrete equilibria that are subject to a grid scale computational instability. Different and stable equilibria were previously constructed by Salmon [J. Marine Res. **57**, 503 (1999)]. The two sets of equilibria differ through a nonhydrodynamic or "ghost" mode that has no direct effect on the hydrodynamic behavior derived in the slowly varying limit. However, Salmon's equilibria eliminate a coupling between hydrodynamic and ghost modes, one that leads to instability with a growth rate increasing with wave number. Previous work has usually assumed that truncated moment expansions lead to stable schemes. Such instabilities have implications for lattice Boltzmann equations that simulate other nonideal equations of state, or that simulate fully compressible, nonisothermal fluids using additional particles.

DOI: 10.1103/PhysRevE.65.036309 PACS number(s): 47.11.+j, 05.20.Dd, 92.20.−h

I. INTRODUCTION

Methods based on lattice Boltzmann equations (LBE) are a promising alternative to conventional numerical methods for simulating fluid flows [1]. The lattice Boltzmann approach replaces the nonlinear differential equations of macroscopic fluid dynamics with a simplified description modeled on the kinetic theory of gases. Hydrodynamic behavior is recovered through the Chapman-Enskog expansion, which exploits a small mean free path approximation to describe slowly varying solutions of the underlying kinetic equations. Lattice Boltzmann methods are straightforward to implement since they involve linear constant coefficient differential operators, and have proved especially effective for simulating flows in complicated geometries and exploiting parallel computer architectures. For these reasons, Salmon [2,3] has advocated the use of lattice Boltzmann methods in oceanography, beginning with a lattice Boltzmann formulation of the shallow water equations [2]. The shallow water equations, describing a thin layer of incompressible fluid with a free surface, are commonly used as a prototype for studying phenomena like wave-vortex interactions that are also present in more complicated systems [4,5].

Although lattice Boltzmann equations for the isothermal Navier-Stokes equations were originally constructed empirically as extensions of lattice gas automata [6] to continuous distribution functions [7,8], it was eventually realized that the most common LBE is equivalent to a systematic truncation of the continuum Boltzmann equation in velocity space [9,10]. This derivation is equivalent to a moment expansion of the continuum Maxwell-Boltzmann equilibrium distribution in tensor Hermite polynomials [11].

However, when the same moment expansion is applied to the shallow water equations, it yields lattice Boltzmann equations that differ from those devised by Salmon [2], and turn out to be rendered useless by an instability on the scale of the computational grid, as illustrated in Fig. 1. The basic difficulty is that the constraints ensuring that a particular lattice Boltzmann scheme reproduces, say, the isothermal Navier-Stokes equations, are insufficient to determine a unique set of equilibrium distributions. In the common two-dimensional, nine speed case the Navier-Stokes or shallow water equations provide only eight independent constraints for the nine unknown equilibria. We find that the remaining degree of freedom must be used to eliminate an instability associated with a nonhydrodynamic mode. This instability is not analytically tractable with the eigenvalue techniques used

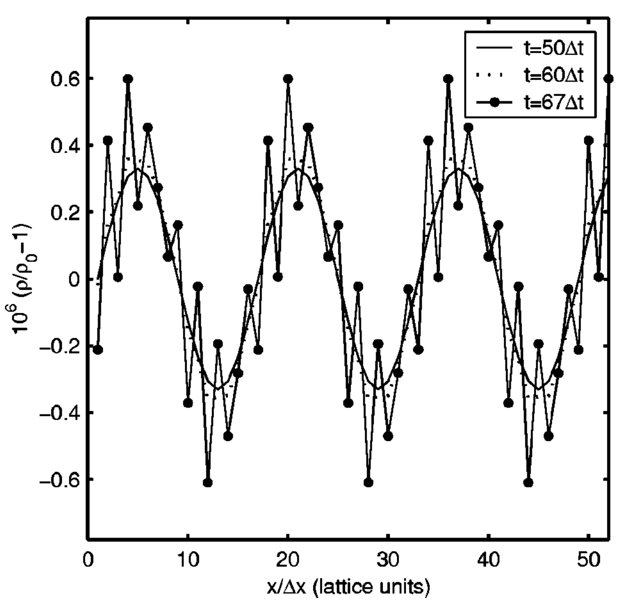

FIG. 1. Growth of a density instability in a two-dimensional shallow water lattice Boltzmann scheme using the Hermite expansion Eq. (23). This is a slice along the line $y=x$. Instability eventually develops on the shortest permitted lengthscale Δx, and then grows rapidly like $\exp(0.36t/\Delta t)$.

*Present address: OCIAM, Mathematical Institute, 24-29 St. Giles', Oxford OX1 3LB, U.K.; electronic address: pdellar@na-net.ornl.gov previously [12,13] on the fully discrete system, so we prefer to treat the instability at the partial differential equation (PDE) level using the concept of nonhydrodynamic or "ghost" variables introduced by Benzi, Succi, and Vergassola [14,15]. A similar approach appeared independently at about the same time by d'Humières [16]. The idea is to augment the evolution equations for the hydrodynamic quantities (density, momentum, and stress) with additional equations to give a complete description of the lattice Boltzmann equation, viewed as a PDE system. We then look for instabilities associated with nonhydrodynamic behavior in these PDEs.

The existence of such instabilities has implications for using lattice Boltzmann equations with modified equilibria to simulate other nonideal equations of state [17], or to include additional physics like magnetic fields [18]. These two previous treatments assumed that equilibria derived from a truncated Hermite expansion with the desired moments would lead to a stable scheme. This work should also be relevant to lattice Boltzmann equations using moment expansions with extra particle speeds for compressible, varying temperature fluids [19–21]. The extra speeds add further undetermined degrees of freedom, even after the heat flux has been specified.

II. SHALLOW WATER EQUATIONS

The two-dimensional shallow water equations are usually written as

$$\partial_t \mathbf{u} + \mathbf{u}\cdot\nabla\mathbf{u} = -g\nabla\rho + \rho^{-1}\nabla\cdot\mathsf{S}, \quad \partial_t\rho + \nabla\cdot(\rho\mathbf{u}) = 0, \tag{1}$$

where $\mathbf{u}=(u,v)$ is the fluid velocity, ρ the free surface height, and the constant g the reduced gravity. Dissipative effects are included via a deviatoric stress tensor S, whose precise form is discussed below. These equations describe a thin layer of incompressible fluid with a free surface, and may be derived by integrating the three-dimensional Navier-Stokes equations in the vertical. We use ρ for the height, rather than h as is common in geophysical fluid dynamics, to highlight the similarity with the Navier-Stokes equations. In fact, if Eqs. (1) are rewritten in conservative form

$$\partial_t(\rho\mathbf{u}) + \nabla\cdot(P\,\mathsf{I} + \rho\mathbf{u}\mathbf{u} - \mathsf{S}) = \mathbf{0}, \quad \partial_t\rho + \nabla\cdot(\rho\mathbf{u}) = 0, \tag{2}$$

P being the pressure, and I the identity matrix. It is also useful to define a momentum flux or stress tensor $\mathbf{\Pi} = P\,\mathsf{I} + \rho\mathbf{u}\mathbf{u} - \mathsf{S}$. In this form, the shallow water equations become identical to the two-dimensional compressible Navier-Stokes equations for a fluid with equation of state $P=\frac{1}{2}g\rho^2$ [22]. For subsequent flexibility we also consider the general barotropic equation of state $P=P(\rho)$, sometimes called "homentropic" [4] to avoid confusion with the usual oceanographic sense of "barotropic" as meaning independent of depth. An isothermal gas, as simulated by the most common lattice Boltzmann equations [1], has $P=c_s^2\rho$, with constant sound speed c_s.

Some diffusive behavior is useful for numerical stability, even though the shallow water equations are normally used to simulate nearly inviscid phenomena, and many applications in geophysical fluid dynamics use algebraic drag terms like $-k\mathbf{u}$ (Rayleigh friction) instead of, or as well as, diffusive stresses [4,5]. For an ideal monatomic gas, $\mathsf{S}=\mu[\nabla\mathbf{u} + (\nabla\mathbf{u})^{\mathsf{T}} - \frac{2}{3}\mathsf{I}\nabla\cdot\mathbf{u}]$, where μ is the dynamic viscosity. Various different forms have been proposed for the dissipative stress in the shallow water equations, as surveyed in Ref. [23], but references [23,24] favor a two-dimensional Newtonian viscous stress, $\mathsf{S}=\mu[\nabla\mathbf{u}+(\nabla\mathbf{u})^{\mathsf{T}} - \frac{1}{2}\mathsf{I}\nabla\cdot\mathbf{u}] + \zeta\mathsf{I}\nabla\cdot\mathbf{u}$, albeit with bulk ($\zeta$) and shear ($\mu$) viscosities proportional to the density ρ to ensure that the dissipation of kinetic energy $\frac{1}{2}\rho|\mathbf{u}|^2$ is sign definite.

III. CONTINUUM KINETIC THEORY

Kinetic theory introduces a distribution function $f(\mathbf{x},\boldsymbol{\xi},t)$, representing the probability density of particles at position $\mathbf{x}$ moving with speed $\boldsymbol{\xi}$ at time t. Macroscopic variables such as fluid density ρ, velocity $\mathbf{u}$, and momentum flux $\mathbf{\Pi}$ are recovered from moments of the distribution function with respect to the microscopic particle velocity $\boldsymbol{\xi}$,

$$\rho = \int f\,d\boldsymbol{\xi}, \quad \rho\mathbf{u} = \int \boldsymbol{\xi} f\,d\boldsymbol{\xi}, \quad \mathbf{\Pi} = \int \boldsymbol{\xi}\boldsymbol{\xi} f\,d\boldsymbol{\xi}. \tag{3}$$

The compressible Navier-Stokes equations may be derived from the continuum Boltzmann Bhatnagar-Gross-Krook (BGK) equation

$$\partial_t f + \boldsymbol{\xi}\cdot\nabla f = -\frac{1}{\tau}(f - f^{(0)}), \tag{4}$$

in a slowly varying limit using the Chapman–Enskog perturbation expansion [25–29]. The computational interest in kinetic theory is largely motivated by the linearity of the differential operator on the left hand side of Eq. (4). On the right hand side of Eq. (4) we have used the BGK approximation [30] to Boltzmann's original binary collision term, in which f relaxes towards an equilibrium distribution $f^{(0)}$ with a single relaxation time τ. The Maxwell-Boltzmann equilibrium distribution in D spatial dimensions is

$$f^{(0)} = \frac{\rho}{(2\pi\Theta)^{D/2}}\exp\left(-\frac{(\boldsymbol{\xi}-\mathbf{u})^2}{2\Theta}\right), \tag{5}$$

where $\rho,\mathbf{u}$ and Θ are the dimensionless macroscopic density, velocity, and temperature determined from f via Eq. (3) and

$$\rho\Theta = \frac{1}{D}\int |\boldsymbol{\xi}-\mathbf{u}|^2 f\,d\boldsymbol{\xi} = \frac{1}{D}\mathrm{Tr}\,\mathbf{\Pi}. \tag{6}$$

We work in units in which the particle masses and Boltzmann's constant are both unity, and velocities are scaled so that the isothermal sound speed $c_s = \Theta^{1/2}$.

Xu [31,32] showed that the shallow water equations could also be cast into continuum kinetic form, using the equilibrium distribution

$$f^{(0)}=\frac{\rho}{(\pi g\rho)^{D/2}}\exp\left(-\frac{(\boldsymbol{\xi}-\mathbf{u})^2}{g\rho}\right), \tag{7}$$

or equivalently by setting $\Theta=\frac{1}{2}g\rho$ in Eq. (5). The ideal gas equation of state $P=\Theta\rho$ then coincides with the shallow water equation of state $P(\rho)=\frac{1}{2}g\rho^2$. Xu [31,32] simulated the inviscid ($\mu=0$) shallow water equations using an upwind finite volume scheme to solve Eqs. (4) and (7).

The "*a priori*" approach [9,10,17,33] attempts to derive to lattice Boltzmann equations from systematic moment, or small Mach number, expansions of the continuum equilibrium distributions such as Eq. (5). In this paper we try to apply this approach to the equilibrium in Eq. (7) for the shallow water equations, and find that the resulting lattice Boltzmann scheme is unstable.

IV. LATTICE BOLTZMANN HYDRODYNAMICS

The simplification leading to the lattice Boltzmann approach restricts the particle velocity $\boldsymbol{\xi}$, previously a continuous variable, to taking values in a discrete set $\{\boldsymbol{\xi}_0,\boldsymbol{\xi}_1,\ldots,\boldsymbol{\xi}_N\}$. The hydrodynamic quantities are now given by discrete moments of the distribution functions $f_i(\mathbf{x},t)=f(\mathbf{x},\boldsymbol{\xi}_i,t)$,

$$\rho=\sum_{i=0}^{N} f_i,\quad \rho\mathbf{u}=\sum_{i=0}^{N}\boldsymbol{\xi}_i f_i,\quad \boldsymbol{\Pi}=\sum_{i=0}^{N}\boldsymbol{\xi}_i\boldsymbol{\xi}_i f_i, \tag{8}$$

which evolve according to the lattice Boltzmann-BGK equation,

$$\partial_t f_i+\boldsymbol{\xi}_i\cdot\nabla f_i=-\frac{1}{\epsilon\tau}(f_i-f_i^{(0)}),\quad \text{for } i=0,\ldots,N. \tag{9}$$

The left hand side is a linear, constant coefficient differential operator obtained by replacing $\boldsymbol{\xi}$ with $\boldsymbol{\xi}_i$ in the continuum Boltzmann-BGK equation (4). We include a formal small parameter ϵ to facilitate the derivation of continuum equations in the limit of small mean free path ($\epsilon\to 0$).

The Chapman–Enskog expansion [25–28] seeks asymptotic solutions of Eq. (9) in the limit $\epsilon\to 0$ by posing a multiple scales expansion of both f and t, but not $\mathbf{x}$, in powers of ϵ

$$f_i=f_i^{(0)}+\epsilon f_i^{(1)}+\epsilon^2 f_i^{(2)}+\cdots,\quad \partial_t=\partial_{t_0}+\epsilon\partial_{t_1}+\cdots. \tag{10}$$

We may think of t_0 and t_1 as advective and diffusive (viscous) time scales, respectively. We impose the two solvability conditions

$$\sum_{i=0}^{N} f_i^{(n)}=\sum_{i=0}^{N}\boldsymbol{\xi}_i f_i^{(n)}=0,\quad \text{for } n=1,2,\ldots. \tag{11}$$

Thus the higher order terms $f^{(1)},f^{(2)},\ldots$, do not contribute to the macroscopic density or momentum. These constraints, which reflect microscopic mass and momentum conservation under collisions, lead to evolution equations for the macroscopic quantities.

A systematic treatment would substitute the expansions (10) into Eq. (9), collect terms at each order, and then take moments. A briefer approach, more in the spirit of this paper, is to take moments of Eq. (9) first

$$\partial_t\rho+\nabla\cdot(\rho\mathbf{u})=0,\quad \partial_t(\rho\mathbf{u})+\nabla\cdot(\boldsymbol{\Pi}^{(0)}+\epsilon\boldsymbol{\Pi}^{(1)}+\cdots)=\mathbf{0}, \tag{12}$$

where $\boldsymbol{\Pi}^{(n)}=\Sigma_{i=0}^{N}\boldsymbol{\xi}_i\boldsymbol{\xi}_i f_i^{(n)}$. The right hand sides vanish in Eq. (12), and ρ and $\mathbf{u}$ require no superscripts, by virtue of the solvability conditions in Eq. (11). We evaluate $\boldsymbol{\Pi}^{(1)}$ using the evolution equation for $\boldsymbol{\Pi}$ derived by applying $\Sigma_{i=0}^{N}\boldsymbol{\xi}_i\boldsymbol{\xi}_i$ to Eq. (9)

$$\partial_t\boldsymbol{\Pi}+\nabla\cdot\left(\sum_{i=0}^{N}\boldsymbol{\xi}_i\boldsymbol{\xi}_i\boldsymbol{\xi}_i f_i\right)=-\frac{1}{\tau}(\boldsymbol{\Pi}-\boldsymbol{\Pi}^{(0)}). \tag{13}$$

At leading order in ϵ this becomes

$$\boldsymbol{\Pi}^{(1)}=-\tau\left(\partial_{t_0}\boldsymbol{\Pi}^{(0)}+\nabla\cdot\sum_{i=0}^{N}\boldsymbol{\xi}_i\boldsymbol{\xi}_i\boldsymbol{\xi}_i f_i^{(0)}\right). \tag{14}$$

The multiple scales expansion of the time derivative in Eq. (10) enables us to replace $\partial_t\boldsymbol{\Pi}^{(0)}$ by $\partial_{t_0}\boldsymbol{\Pi}^{(0)}$ to sufficient accuracy. The latter may be expressed in terms of the known quantities $\partial_{t_0}\rho$ and $\partial_{t_0}(\rho\mathbf{u})$

$$\begin{aligned}\partial_{t_0}\boldsymbol{\Pi}^{(0)}&=\partial_{t_0}(P(\rho)\mathsf{I}+\rho\mathbf{u}\mathbf{u})\\&=\mathsf{I}\frac{dP}{d\rho}\partial_{t_0}\rho+\mathbf{u}\partial_{t_0}(\rho\mathbf{u})+\partial_{t_0}(\rho\mathbf{u})\mathbf{u}-\mathbf{u}\mathbf{u}\partial_{t_0}\rho\end{aligned} \tag{15}$$

as evaluated in Appendix A. We find that $\boldsymbol{\Pi}^{(1)}$ is a dissipative stress, equivalent to that in a Newtonian fluid, for the isothermal Navier-Stokes equations, but $\boldsymbol{\Pi}^{(1)}$ is not a Newtonian viscous stress for other barotropic equations of state. The dynamic viscosity μ is related to the collision time scale τ in Eq. (9) via $\mu=\tau\theta\rho$.

Equation (9) is usually implemented computationally using the fully discrete system [1,33]

$$\begin{aligned}&\overline{f_i}(\mathbf{x}+\boldsymbol{\xi}_i\Delta t,t+\Delta t)-\overline{f_i}(\mathbf{x},t)\\&\quad=-\frac{\Delta t}{\tau+\Delta t/2}(\overline{f_i}(\mathbf{x},t)-f_i^{(0)}(\mathbf{x},t)),\end{aligned} \tag{16}$$

where the $\overline{f_i}$ are defined by

$$\overline{f_i}(\mathbf{x},t)=f_i(\mathbf{x},t)+\frac{\Delta t}{2\tau}(f_i(\mathbf{x},t)-f_i^{(0)}(\mathbf{x},t)). \tag{17}$$

The solvability conditions imply that this substitution leaves the density and momentum unchanged, so that

$$\rho=\sum_{i=0}^{N}\overline{f_i},\quad \rho\mathbf{u}=\sum_{i=0}^{N}\boldsymbol{\xi}_i\overline{f_i} \tag{18}$$

so the $f_i^{(0)}$ may be computed directly from the $\overline{f_i}$, making the f_i redundant. Equation (16) is algebraically identical to a

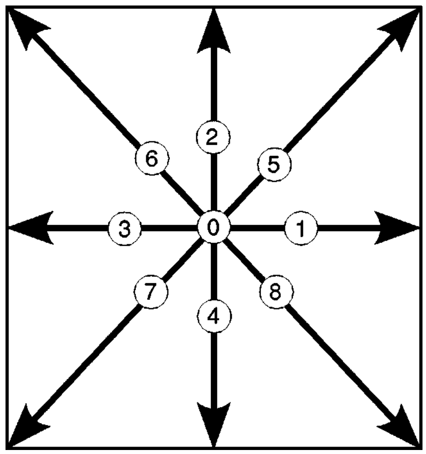

FIG. 2. The nine particle speeds $\boldsymbol{\xi}_i$ in the two-dimensional square lattice. We choose units in which $|\boldsymbol{\xi}_1|=1$, and $|\boldsymbol{\xi}_5|=\sqrt{2}$.

discrete form of Eq. 9 with second order accuracy, i.e., $O(\Delta t^2)$ error, obtained by integrating the right hand side along characteristics for a time interval Δt using the trapezium rule. The change of variables (17) yields an explicit scheme, expressing $\overline{f_i}$ at time $t+\Delta t$ explicitly in terms of quantities known at time t.

V. NINE SPEED EQUILIBRIA

The equilibria $f_i^{(0)}$ and speeds $\boldsymbol{\xi}_i$ must be constructed to recover the desired continuum equations in the limit of slow variations in $\mathbf{x}$ and t. In particular, the first few moments of the equilibria must be

$$\sum_{i=0}^{N} f_i^{(0)}=\rho, \quad \sum_{i=0}^{N} \boldsymbol{\xi}_i f_i^{(0)}=\rho\mathbf{u},$$
$$\boldsymbol{\Pi}^{(0)}=\sum_{i=0}^{N} \boldsymbol{\xi}_i\boldsymbol{\xi}_i f_i^{(0)}=P(\rho)\mathsf{I}+\rho\mathbf{u}\mathbf{u} \tag{19}$$

making the leading order ($\epsilon=0$) Eqs. (12) equivalent to the inviscid ($\mu=0$) continuum equations.

The most common lattice Boltzmann equations for simulating the two-dimensional isothermal Navier-Stokes use nine particle speeds located on a square lattice [1], although earlier work employed six or seven particle speeds located on a hexagon [6,7,12]. The equilibria are given by

$$f_i^{(0)}=w_i\rho\left(1+3\boldsymbol{\xi}_i\cdot\mathbf{u}+\frac{9}{2}(\boldsymbol{\xi}_i\cdot\mathbf{u})^2-\frac{3}{2}\mathbf{u}^2\right) \tag{20}$$

in units where the (constant) temperature $\Theta=\frac{1}{3}$, and the weight factors w_i are [1,8,9]

$$w_i=\begin{cases} 4/9, & \mathrm{i}=0,\\ 1/9, & \mathrm{i}=1,2,3,4,\\ 1/36, & \mathrm{i}=5,6,7,8. \end{cases} \tag{21}$$

The components of the particle speeds $\boldsymbol{\xi}_i$ take integer values $\{-1,0,1\}$, forming a square lattice as shown in Fig. 2. These distribution functions were originally constructed as polynomials in $\mathbf{u}$ whose coefficients are arbitrary functions of ρ. The moments (19) impose constraints on the coefficients, and the form of the viscous stress imposes further constraints (see Appendix A). However, at least one coefficient remains arbitrary with nine speeds, and more with 13, 16, or 17 speeds [19].

More recently, a systematic derivation was proposed by He and Luo [9], based on the observation that the continuum Maxwell-Boltzmann equilibrium (5) may be expanded as

$$f^{(0)}=\rho w(\boldsymbol{\xi})\left(1+\frac{\boldsymbol{\xi}\cdot\mathbf{u}}{\Theta}+\frac{(\boldsymbol{\xi}\cdot\mathbf{u})^2}{2\Theta^2}-\frac{\mathbf{u}^2}{2\Theta}\right)+O(\mathbf{u}^3), \tag{22}$$

where $w(\boldsymbol{\xi})=(2\pi\Theta)^{-D/2}\exp[-\boldsymbol{\xi}^2/(2\Theta)]$. This was originally motivated as a small Mach number expansion, valid for $|\mathbf{u}|\ll|\boldsymbol{\xi}|$, but it is equivalent to a moment expansion in tensor Hermite polynomials. The equilibria (20) then followed from Eq. (22) by replacing the continuum weight function $w(\boldsymbol{\xi})$ by discrete weights w_i obtained from a two-dimensional Gaussian quadrature formula, chosen to make every discrete moment appearing in Sec. IV identical in value to its continuum analogue in classical kinetic theory. The choice $\Theta=\frac{1}{3}$ causes the Gaussian quadrature points in x and y to be the integers $\{-1,0,1\}$, and causes the polynomials in Eqs. (22) and (20) to coincide.

Applied to the shallow water equations, or to an arbitrary barotropic equation of state $P(\rho)$, the same moment expansion leads to the equilibria

$$f_i^{(0)}=w_i\left(\rho+\frac{1}{\theta}(\rho\mathbf{u})\cdot\boldsymbol{\xi}_i+\frac{1}{2\theta^2}[(P(\rho)-\theta\rho)\mathsf{I}+\rho\mathbf{u}\mathbf{u}]:(\boldsymbol{\xi}_i\boldsymbol{\xi}_i-\theta\mathsf{I})\right). \tag{23}$$

We use a lower case θ to emphasize that $\theta=\frac{1}{3}$ is now a constant reference temperature, equivalent to a velocity scale set by the particle speeds, rather than a local fluid temperature that may be spatially varying. Each term in Eq. (23) involves one of the tensor Hermite polynomials $1,\boldsymbol{\xi}_i$, and $\boldsymbol{\xi}_i\boldsymbol{\xi}_i-\theta\mathsf{I}$, contracted with the required Hermite moment $\rho,\rho\mathbf{u}$, and $\boldsymbol{\Pi}^{(0)}-\theta\rho\mathsf{I}=(P(\rho)-\theta\rho)\mathsf{I}+\rho\mathbf{u}\mathbf{u}$, respectively. The tensor Hermite polynomials have the property of being orthogonal with respect to both a discrete and a continuous inner product (see Sec. VI). Since the required Hermite moments are already known, it is actually unnecessary to construct a continuum distribution function first, but Eq. (5) with $\Theta=P(\rho)/\rho$ would suffice. The equilibria in Eq. (23) take a particularly simple form for the isothermal Navier-Stokes equations, with $P(\rho)=\theta\rho$, as the isotropic pressure term in square brackets $[\cdot]$ vanishes.

The same expansion (23) may also be obtained through a small Mach number expansion of Xu's continuum distribution function (7). As the density ρ appears in the exponent it is necessary to consider a nearly uniform density, $\rho=\rho_0+\mathrm{Ma}^2\rho'$, as well as scaling $\mathbf{u}=O(\mathrm{Ma})$, to obtain

$$\frac{\rho}{(\pi g\rho)}\exp\left(-\frac{(\boldsymbol{\xi}-\mathbf{u})^2}{g\rho}\right)=\rho_0 w(\boldsymbol{\xi})\left(1+\frac{\boldsymbol{\xi}\cdot\mathbf{u}}{\Theta}+\frac{(\boldsymbol{\xi}\cdot\mathbf{u})^2}{2\Theta^2}-\frac{\mathbf{u}^2}{2\Theta}+\frac{(\rho-\rho_0)\boldsymbol{\xi}^2}{2\Theta}\right)+O(\mathrm{Ma}^3), \quad (24)$$

where $\Theta=\frac{1}{2}g\rho_0$. Rearranging to replace ρ_0 by ρ as the premultiplier, we may also obtain

$$\frac{\rho}{(\pi g\rho)}\exp\left(-\frac{(\boldsymbol{\xi}-\mathbf{u})^2}{g\rho}\right)=\rho w(\boldsymbol{\xi})\left(1+\frac{\boldsymbol{\xi}\cdot\mathbf{u}}{\Theta}+\frac{(\boldsymbol{\xi}\cdot\mathbf{u})^2}{2\Theta^2}-\frac{\mathbf{u}^2}{2\Theta}+(\rho-\rho_0)\left[\frac{\boldsymbol{\xi}^2}{2\Theta}-1\right]\right)+O(\mathrm{Ma}^3), \quad (25)$$

which coincides with the moment expansion (23) above on substituting $\boldsymbol{\xi}=\boldsymbol{\xi}_i$ and $w(\boldsymbol{\xi}_i)=w_i$. In fact, the assumption that $\rho=\rho_0+O(\mathrm{Ma}^2)$ turns out to be unduly restrictive, and the lattice Boltzmann scheme below successfully simulates flows with $O(1)$ density fluctuations.

Unfortunately, the lattice Boltzmann equation for the shallow water equations ($P=\frac{1}{2}g\rho^2$) with these equilibria turns out to be linearly unstable to a rapidly growing zigzag mode at the grid scale, rendering it useless for numerical simulations. However, a stable and useful lattice Boltzmann formulation for shallow water has already been devised by Salmon [2], that uses the alternative equilibria

$$f_0^{(0)}=\rho+w_0\rho\left(-\frac{15}{8}g\rho-\frac{3}{2}\mathbf{u}^2\right), \quad (26a)$$

$$f_i^{(0)}=w_i\rho\left(\frac{3}{2}g\rho+3\boldsymbol{\xi}_i\cdot\mathbf{u}+\frac{9}{2}(\boldsymbol{\xi}_i\cdot\mathbf{u})^2-\frac{3}{2}\mathbf{u}^2\right), \quad \text{for } i\neq 0, \quad (26b)$$

where Salmon chose an otherwise arbitrary coefficient so that Eq. (26b) takes the same form for both $|\boldsymbol{\xi}_i|=1$ and $|\boldsymbol{\xi}_i|=\sqrt{2}$ types of particles (see Fig. 2).

This casts doubt on the utility of the Hermite polynomial expansion at constructing equilibrium distribution functions for systems other than the isothermal Navier-Stokes equations. In fact, Salmon's equilibria (26a,b) may be rewritten in the form

$$f_i^{(0)}=w_i\left(\rho+\frac{1}{\theta}(\rho\mathbf{u})\cdot\boldsymbol{\xi}_i+\frac{1}{2\theta^2}\times[(P(\rho)-\theta\rho)\mathsf{I}+\rho\mathbf{u}\mathbf{u}]:(\boldsymbol{\xi}_i\boldsymbol{\xi}_i-\theta\mathsf{I})\right)+w_i g_i\left(\frac{1}{4}\rho-\frac{3}{8}g\rho^2\right), \quad (27)$$

which differs from the truncated Hermite expansion (23) only through a multiple of the "ghost vector" $g_i=(1,-2,-2,-2,-2,4,4,4,4)^{\mathsf{T}}$. This vector is orthogonal in a discrete sense to the Hermite polynomials appearing in Eqs. (23) and (27), so the modification to Eq. (27) leaves the continuity and momentum Eqs. (12) unchanged up to $O(\epsilon)$ in the Chapman–Enskog expansion. This particular choice for the otherwise arbitrary function $F(\rho,|\mathbf{u}|)$ multiplying $w_i g_i$ is determined in Sec. VI below, in that it eliminates an instability due to cross coupling to some nonhydrodynamic "ghost modes" present in the lattice Boltzmann equation.

VI. NONHYDRODYNAMIC GHOST VARIABLES

In principle the equilibrium distribution functions $f_i^{(0)}$ for the nine particle speeds are nine independent arbitrary functions. The constraints (19) on the first three moments comprise only six independent constraints, since the symmetric second rank tensor $\mathbf{\Pi}^{(0)}$ has only three independent components in two dimensions. In this section we develop a treatment of the remaining three degrees of freedom, later identified with nonhydrodynamic "ghost" variables.

Ghost variables were introduced by Benzi, Succi, and Vergassola [14,15] for an earlier form of lattice Boltzmann equation

$$\partial_t f_i+\boldsymbol{\xi}_i\cdot\nabla f_i=-\frac{1}{\tau}\Omega_{ij}(f_j-f_j^{(0)}), \quad \text{for } i=0,\ldots,N, \quad (28)$$

where the 9×9 matrix Ω_{ij} was obtained by linearizing a quadratic collision operator of the kind used in lattice gas cellular automata [6]. A similar treatment appeared about the same time by d'Humières [16]. Hydrodynamic and ghost vectors arose naturally in both these treatments as eigenvectors of the collision matrix Ω_{ij}. The Bhatnagar-Gross-Krook (BGK) approximation [30] used in Eqs. (4) and (9) takes $\Omega_{ij}=\delta_{ij}$, so all departures from equilibrium decay at the same rate. The BGK approximation is now almost universally employed, since it eliminates various artifacts like a velocity-dependent pressure that plagued earlier models [1]. Any lattice vector is an eigenvector of the BGK collision operator, making the choice of basis somewhat arbitrary. For instance, Lallemand and Luo [13], following Ref. [16], used a different basis that is orthogonal with respect to the unweighted inner product $\langle f,h\rangle=\Sigma_{i=0}^8 f_i h_i$ instead of the weighted inner product in Eq. (30). This basis leads to a rather unnatural equation for the normal stress difference $\Pi_{xx}-\Pi_{yy}$ in place of Eq. (35b).

The expressions (23) and (27) for the equilibria involve the first three tensor Hermite polynomials $1,\boldsymbol{\xi}$ and $\boldsymbol{\xi}\boldsymbol{\xi}-\theta\mathsf{I}$, with coefficients depending on the hydrodynamic variables ρ and $\mathbf{u}$. The components of the tensor Hermite polynomials comprise the six polynomials $1,\xi_{ix},\xi_{iy},\xi_{ix}^2-\theta,\xi_{ix}\xi_{iy}$ and $\xi_{iy}^2-\theta$, each of which may be regarded as a nine-dimensional lattice vector, p say, with components $(p_0,p_1,\ldots,p_8)$ corresponding to the polynomial evaluated at the lattice points $\boldsymbol{\xi}_i$. Written out in full, these vectors are

$$1_i=(1,1,1,1,1,1,1,1,1)^{\mathsf{T}},$$

$$\xi_{ix}=(0,1,0,-1,0,1,-1,-1,1)^{\mathsf{T}},$$

$$\xi_{iy} = (0,0,1,0,-1,1,1,-1,-1)^{\mathsf{T}},$$

$$\xi_{ix}^2 - \theta 1_i = \frac{1}{3}(-1,2,-1,2,-1,2,2,2,2)^{\mathsf{T}}, \qquad (29)$$

$$\xi_{ix}\xi_{iy} = (0,0,0,0,0,1,-1,1,-1)^{\mathsf{T}},$$

$$\xi_{iy}^2 - \theta 1_i = \frac{1}{3}(-1,-1,2,-1,2,2,2,2,2)^{\mathsf{T}}.$$

These six lattice vectors are orthogonal with respect to the inner product defined by the weights w_i. In other words

$$\langle p,q\rangle = \sum_{i=0}^{8} w_i p_i q_i = 0 \quad \text{for} \quad p \neq q, \qquad (30)$$

where "$p=q$" means "$p_i = q_i$ for $i=0,\ldots,8$." This is the discrete analogue of the continuous orthogonality relation satisfied by the original polynomials

$$\int w(\boldsymbol{\xi}) p(\boldsymbol{\xi}) q(\boldsymbol{\xi}) d\boldsymbol{\xi} = 0 \quad \text{for} \quad p \neq q, \qquad (31)$$

where $w(\boldsymbol{\xi}) = (2\pi\theta)^{-1}\exp[-\boldsymbol{\xi}^2/(2\theta)]$ in two dimensions $(D=2)$ as in Sec. V. Equation (30) follows from Eq. (31) using the two-dimensional Gaussian quadrature formula

$$\int w(\boldsymbol{\xi}) p(\boldsymbol{\xi}) q(\boldsymbol{\xi}) d\boldsymbol{\xi} = \sum_{i=0}^{8} w_i p(\boldsymbol{\xi}_i) q(\boldsymbol{\xi}_i) = \sum_{i=0}^{8} w_i p_i q_i, \qquad (32)$$

provided the product $p(\boldsymbol{\xi})q(\boldsymbol{\xi})$ is a polynomial of degree five or less in ξ_x and ξ_y [34,9,33]. It may be helpful to draw an analogy with the trigonometric functions $\sin(nx)$ and $\cos(nx)$, as they also satisfy both discrete and continuous orthogonality relations on the periodic interval $[0,2\pi]$.

The six orthogonal lattice vectors in Eqs. (29) may be extended to form an orthogonal *basis* for $\mathbb{R}^9$ with the addition of three more vectors, conveniently expressed as $g_i, g_i\xi_{ix}$, and $g_i\xi_{iy}$, where

$$g_i\xi_{ix} = (0,-2,0,2,0,4,-4,-4,4)^{\mathsf{T}},$$

$$g_i\xi_{iy} = (0,0,-2,0,2,4,4,-4,-4)^{\mathsf{T}}, \qquad (33)$$

$$g_i = (1,-2,-2,-2,-2,4,4,4,4)^{\mathsf{T}},$$

with g_i as in Sec. V above. Associated with these three extra vectors are three extra moments, named "ghost variables" by Benzi, Succi, and Vergassola [14,15]

$$N = \sum_{i=0}^{8} g_i f_i, \quad \mathbf{J} = \sum_{i=0}^{8} g_i \boldsymbol{\xi}_i f_i \qquad (34)$$

by analogy with the hydrodynamic moments $\rho, \rho\mathbf{u}$ and $\boldsymbol{\Pi}$ defined previously. The hydrodynamic equations

$$\partial_t \rho + \nabla\cdot(\rho\mathbf{u}) = 0, \quad \partial_t(\rho\mathbf{u}) + \nabla\cdot\boldsymbol{\Pi} = \mathbf{0}, \qquad (35a)$$

$$\partial_t \boldsymbol{\Pi} + \nabla\cdot\left(\sum_{i=0}^{8} \boldsymbol{\xi}_i\boldsymbol{\xi}_i\boldsymbol{\xi}_i f_i\right) = -\frac{1}{\tau}(\boldsymbol{\Pi} - \boldsymbol{\Pi}^{(0)}) \qquad (35b)$$

comprising six independent equations since $\boldsymbol{\Pi}$ is symmetric, may thus be augmented by three ghost component equations

$$\partial_t N + \nabla\cdot\mathbf{J} = -\frac{1}{\tau}(N - N^{(0)}),$$

$$\partial_t \mathbf{J} + \nabla\cdot\left(\sum_{i=0}^{8} g_i\boldsymbol{\xi}_i\boldsymbol{\xi}_i f_i\right) = -\frac{1}{\tau}(\mathbf{J} - \mathbf{J}^{(0)}) \qquad (36)$$

to give a complete description of the nine speed lattice Boltzmann equation (9). In other words, the nine quantities f_i may be reconstructed from the nine independent components of $\rho, \mathbf{u}, \boldsymbol{\Pi}, N$, and $\mathbf{J}$ as

$$f_i = w_i\left(\rho + \frac{1}{\theta}(\rho\mathbf{u})\cdot\boldsymbol{\xi}_i + \frac{1}{2\theta^2}(\boldsymbol{\Pi} - \theta\rho\mathsf{I}):(\boldsymbol{\xi}_i\boldsymbol{\xi}_i - \theta\mathsf{I})\right) + w_i g_i\left(\frac{1}{4}N + \frac{3}{8}\boldsymbol{\xi}_i\cdot\mathbf{J}\right) \qquad (37)$$

and the lattice Boltzmann equation (9) may be reconstructed by combining the hydrodynamic equations (35a,b) with the ghost variable equations (36). This procedure is thus equivalent to a linear change of variables in the lattice Boltzmann equation, one chosen to separate the intended hydrodynamic behavior from unintentional ghost behavior.

The most general equilibria with the required first three moments (19) are therefore

$$f_i^{(0)} = w_i\left(\rho + \frac{1}{\theta}(\rho\mathbf{u})\cdot\boldsymbol{\xi}_i + \frac{1}{2\theta^2}[\rho\mathbf{u}\mathbf{u} + (P(\rho) - \theta\rho)\mathsf{I}]:(\boldsymbol{\xi}_i\boldsymbol{\xi}_i - \theta\mathsf{I})\right) + w_i g_i\left(\frac{1}{4}N^{(0)} + \frac{3}{8}\boldsymbol{\xi}_i\cdot\mathbf{J}^{(0)}\right), \qquad (38)$$

where $N^{(0)}$ and $\mathbf{J}^{(0)}$ may be arbitrary scalar and vector functions, respectively. The components of the tensors $\boldsymbol{\xi}_i\boldsymbol{\xi}_i\boldsymbol{\xi}_i$ and $g_i\boldsymbol{\xi}_i\boldsymbol{\xi}_i$ appearing in Eqs. (35b) and (36) may be expressed in terms of the nine basis lattice vectors as

$$g_i\xi_{ix}\xi_{ix} = 2(\xi_{iy}\xi_{iy} - \theta 1_i) + \frac{2}{3}g_i, \qquad g_i\xi_{ix}\xi_{iy} = 4\xi_{ix}\xi_{iy}, \qquad (39a)$$

$$\xi_{ix}\xi_{ix}\xi_{ix} = \xi_{ix}, \qquad \xi_{ix}\xi_{ix}\xi_{iy} = \frac{1}{3}\xi_{iy} + \frac{1}{6}g_i\xi_{iy} \qquad (39b)$$

and their permutations in x and y. Recall that we are using the term "lattice vector" to denote a collection of nine values at the nine lattice points, so the xx component of a tensor, say, comprises a lattice vector labeled by the index i. The relations (39a,b) are responsible for cross coupling between the hydrodynamic and ghost variables. In particular $\mathbf{J}$ appears in the nonequilibrium stress via Eqs. (39b) and (35b)

$$\partial_t \Pi_{xx} + \partial_x(\rho u_x) + \partial_y\left(\frac{1}{3}\rho u_y + \frac{1}{6}J_y\right) = -\frac{1}{\tau}(\Pi_{xx} - \Pi_{xx}^{(0)}), \tag{40a}$$

$$\partial_t \Pi_{xy} + \partial_x\left(\frac{1}{3}\rho u_y + \frac{1}{6}J_y\right) + \partial_y\left(\frac{1}{3}\rho u_x + \frac{1}{6}J_x\right) = -\frac{1}{\tau}(\Pi_{xy} - \Pi_{xy}^{(0)}) \tag{40b}$$

(similarly for Π_{yy}), which are equivalent to the components Eq. (13). Similarly, the second of Eqs. (36) becomes

$$\partial_t J_x + \partial_x\left(2\Pi_{yy} - \frac{2}{3}\rho + \frac{2}{3}N\right) + 4\partial_y \Pi_{xy} = -\frac{1}{\tau}(J_x - J_x^{(0)}), \tag{41a}$$

$$\partial_t J_y + 4\partial_x \Pi_{xy} + \partial_y\left(2\Pi_{xx} - \frac{2}{3}\rho + \frac{2}{3}N\right) = -\frac{1}{\tau}(J_y - J_y^{(0)}). \tag{41b}$$

Although the nine speed lattice has sufficient symmetry to recover the isotropic Navier-Stokes equations at the first two orders in the Chapman-Enskog expansion, these ghost equations are not themselves isotropic.

To summarize, the lattice Boltzmann equation (9) separates into the set of equations (35a, 40a,b, 36, 41a,b) for $\rho, \rho\mathbf{u}, \mathbf{\Pi}, N$ and $\mathbf{J}$, respectively, in the orthogonal basis given by Eqs. (29) and (33). The variables $\mathbf{\Pi}^{(0)}, N^{(0)}$ and $\mathbf{J}^{(0)}$ appearing in Eqs. (40a,b, 36, 41a,b) are determined by the equilibrium distribution in Eq. (38). The leading order stress $\mathbf{\Pi}^{(0)} = P(\rho)\mathsf{I} + \rho\mathbf{uu}$ is determined by the equation of state, but $N^{(0)}$ and $\mathbf{J}^{(0)}$ remain arbitrary.

We must choose $\mathbf{J}^{(0)} = \mathbf{0}$ to avoid interfering with the leading order viscous stress $\mathbf{\Pi}^{(1)}$ (see Appendix A below) via the cross coupling in Eq. (39b) involving $\xi_{ix}\xi_{ix}\xi_{iy}$. Thus the leading order equation for the ghost variable $\mathbf{J}$ becomes

$$\nabla \cdot \begin{pmatrix} 2\rho u_y^2 & 4\rho u_x u_y \\ 4\rho u_x u_y & 2\rho u_x^2 \end{pmatrix} + 2\nabla\left(P(\rho) - \frac{1}{3}\rho + \frac{1}{3}N^{(0)}\right) = -\frac{1}{\tau}\mathbf{J}^{(1)} \tag{42}$$

using Eq. (39a), by analogy with equation Eq. (14) for $\mathbf{\Pi}^{(1)}$. However, $N^{(0)}$ so far remains arbitrary, and must be determined by some criterion other than the form of the continuum equations at viscous order in the Chapman-Enskog expansion, since $N^{(0)}$ does not appear in these equations.

VII. DENSITY-DRIVEN INSTABILITY MECHANISM

The first term in Eq. (42) is present in the usual lattice Boltzmann scheme for the isothermal Navier-Stokes equations, as in [8–10,1], and is found to be innocuous there as the scheme is stable even for high Reynolds numbers (small viscosity). More concretely, the first term is $O(\mathrm{Ma}^2)$ in the usual scaling where $\mathbf{u} = O(\mathrm{Ma})$. The second, gradient term was not present in the isothermal Navier-Stokes case, since $P = (1/3)\rho$ and $N^{(0)} = 0$. Since $\nabla\rho$ may be $O(1)$ in the shallow water equations, this term is also much larger than the first term. These observations strongly suggest that this term is responsible for the observed instability, which is supported by the fact that Salmon's choice [2] for the undetermined function $N^{(0)} = \rho - (3/2)g\rho^2 = \rho - 3P(\rho)$ in Eq. (27) eliminates both this additional term and the instability.

To illustrate the instability mechanism, we consider small perturbations about a rest state with uniform density. Discarding the first term on the left hand side of Eq. (42), which is $O(\mathrm{Ma}^2)$ smaller than the second term, we obtain

$$\mathbf{J}^{(1)} = -2\tau\nabla\left(P(\rho) - \frac{1}{3}\rho + \frac{1}{3}N^{(0)}\right) = -2\tau\nabla Q(\rho) \tag{43}$$

defining $Q(\rho)$ as a convenient shorthand. Discarding terms involving $\rho\mathbf{u}$ and $\partial_{t_0}\mathbf{\Pi}^{(0)}$ from Eqs. (40a,b), we find

$$\Pi_{xx} = P(\rho) + \frac{\tau^2}{3}\frac{\partial^2 Q}{\partial y^2}, \quad \Pi_{xy} = \frac{2\tau^2}{3}\frac{\partial^2 Q}{\partial x \partial y},$$

$$\Pi_{yy} = P(\rho) + \frac{\tau^2}{3}\frac{\partial^2 Q}{\partial x^2}. \tag{44}$$

These simplifications are only intended to highlight the instability mechanism associated with the gradient term in Eq. (42). As explained below, any quantitative treatment must recognize that the computational system is only a discrete approximation to the PDE system.

The continuity and momentum Eqs. (35a) may be differentiated with respect to time, without further approximation, to obtain

$$\frac{\partial^2\rho}{\partial t^2} = -\frac{\partial^2(\rho u_x)}{\partial x \partial t} - \frac{\partial^2(\rho u_y)}{\partial y \partial t} = \frac{\partial^2 \Pi_{xx}}{\partial x^2} + 2\frac{\partial^2 \Pi_{xy}}{\partial x \partial y} + \frac{\partial^2 \Pi_{yy}}{\partial y^2} = \nabla^2 P(\rho) + 2\tau^2\frac{\partial^4 Q(\rho)}{\partial x^2 \partial y^2}. \tag{45}$$

If $dQ/d\rho > 0$, this equation is linearly unstable to perturbations of the form $\rho(x,y,t) = \rho_0 + \rho' \exp(\sigma t + ixk_x + iyk_y)$ about a uniform state with density ρ_0. The growth rate σ is determined by

$$\sigma^2 = -(k_x^2 + k_y^2)\frac{dP}{d\rho}\bigg|_{\rho=\rho_0} + 2\tau^2 k_x^2 k_y^2 \frac{dQ}{d\rho}\bigg|_{\rho=\rho_0}. \tag{46}$$

In fact, the equation is ill posed when $dQ/d\rho > 0$, because the growth rate increases faster than linearly with wave number, $|\sigma| \propto |\mathbf{k}|^2$. If $dQ/d\rho < 0$ the Q term only leads to high frequency oscillations, i.e., σ purely imaginary, with frequency proportional to $k_x k_y$, rather than frequency proportional to $|\mathbf{k}|$ like the sound waves associated with the pressure term in Eq. (46). This is the case for the equilibria based on a Hermite expansion for the shallow water equations, where $Q(\rho)=-\frac{1}{3}\rho+\frac{1}{2}g\rho^2$, and $dQ/d\rho=-\frac{1}{3}+O(\mathrm{Ma}^2/\mathrm{Fr}^2)$ is typically negative. However, it is easy to suppose that the discrete system would in turn be unstable for such high frequency waves, based on a Courant-Friedrichs-Lewy stability criterion, so high frequency waves in the PDEs would, in fact, appear as growing modes in the discrete system.

The scaling $|\sigma|\propto|\mathbf{k}|^2$ explains why numerical simulations exhibit an instability on the scale of the computational grid, since this analysis predicts that the fastest growing mode is the shortest mode permitted, although strictly the description of the discrete computational system as a set of partial differential equations breaks down at these scales. The instability associated with Q is only present if both k_x and k_y are nonzero, which explains why the one-dimensional version of the Hermite expansion shallow water lattice Boltzmann scheme is stable.

VIII. EIGENVALUE PROBLEM

For a quantitative treatment of the instability, we consider an eigenvalue problem as in Refs. [12,13,35] for the the linearized response of the fully discrete system (16) to plane waves of the form

$$\overline{f_i}(\mathbf{x},t)=f_i^{(0)}|_{\rho=\rho_0,\mathbf{u}=0}+h_i\exp(i\mathbf{k}\cdot\mathbf{x}+\sigma t), \qquad (47)$$

where the h_i are small constants. We have linearized around a uniform rest state with $\rho=\rho_0$ and $\mathbf{u}=\mathbf{0}$ for simplicity. In this section we use lattice units in which $\Delta x=\Delta t=1$. The continuum limit then corresponds to $|\mathbf{k}|\to 0$, for which presumably $\sigma\to 0$, too. Substituting into Eq. (16) we obtain

$$[\exp(\sigma+i\mathbf{k}\cdot\boldsymbol{\xi}_i)-1]h_i=-\frac{1}{\tau+1/2}\mathsf{L}_{ij}h_j, \qquad (48)$$

which is an eigenvalue problem for e^{σ}, with h_i the associated eigenvector. The 9×9 matrix L_{ij} is the result of linearizing the BGK collision operator $\overline{f_i}-f_i^{(0)}$ around the rest state ($\rho=\rho_0,\mathbf{u}=\mathbf{0}$), recalling that $f_i^{(0)}$ depends implicitly and nonlinearly on the $\overline{f_i}$ via ρ and $\mathbf{u}$. In general, the eigenvalue problem is not analytically tractable, involving a ninth degree polynomial that does not readily factorize, and has to be solved numerically, for instance, by the so-called QR algorithm [36]. The parameter space is also rather large, involving at least the wave vector $\mathbf{k}$, the relaxation time τ (equivalent to the viscosity), the derivative of pressure $dP/d\rho$ evaluated at the background density ρ_0, and also $dQ/d\rho$ at $\rho=\rho_0$ (or equivalently the parameter λ from Appendix B). In principle we should also consider background states with a nonzero uniform velocity $\mathbf{u}_0$ as well, adding another two parameters. The vectors $\mathbf{k}$ and $\mathbf{u}_0$ must be kept as general vectors because the ghost equations are anisotropic.

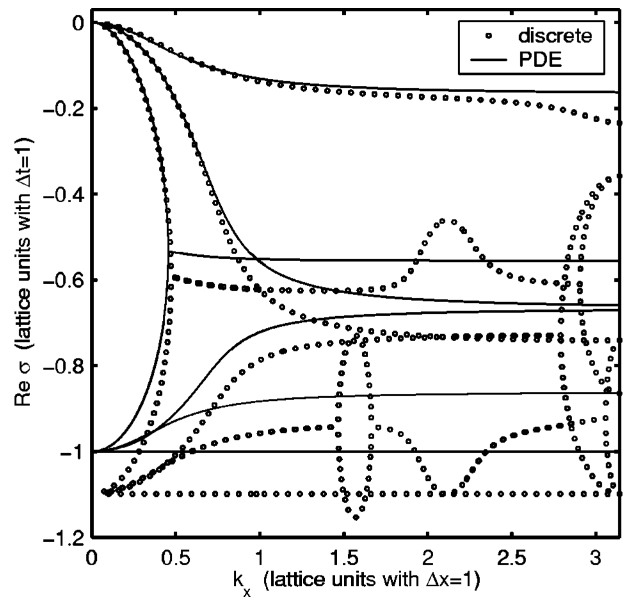

FIG. 3. Eigenvalues of the systems (48) and (49) for $k_x=k_y$, and parameters $\tau=1,P=0$, and $Q=-\frac{1}{3}\rho$ (as in the Hermite expansion). All modes are stable ($\mathrm{Re}\,\sigma\leqslant 0$) in both the continuum (—) and discrete (●) systems.

In the continuum limit, where $\mathbf{k}$ and σ are both small, and τ is large (compared with the time step Δt) the eigenvalues of the discrete system (48) should coincide with the analogous eigenvalues of the lattice Boltzmann PDE system (9)

$$(\sigma+i\mathbf{k}\cdot\boldsymbol{\xi}_i)h_i=-\frac{1}{\tau}\mathsf{L}_{ij}h_j. \qquad (49)$$

Figures 3 and 4 show the real parts of the eigenvalues of

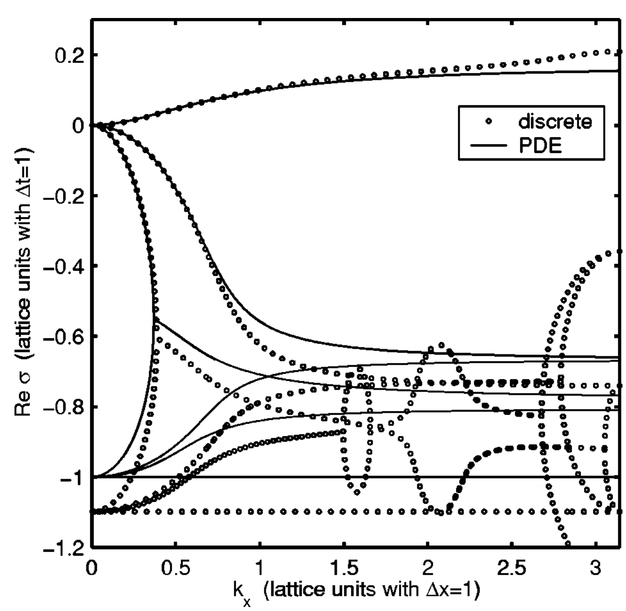

FIG. 4. Eigenvalues of the systems (48) and (49) for $k_x=k_y$, and parameters $\tau=1,P=0,Q=\frac{1}{3}\rho$. One mode is unstable ($\mathrm{Re}\,\sigma>0$) in both the continuum (—) and discrete (●) systems.

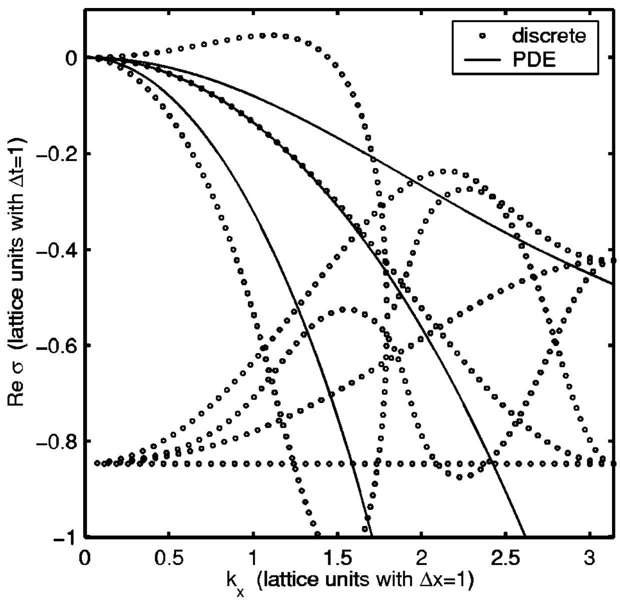

FIG. 5. Eigenvalues of the systems (48) and (49) for $k_x=k_y$, and parameters $\tau=0.2,P=0,Q=-\frac{1}{3}\rho$ (as in the Hermite expansion). One mode becomes unstable ($\mathrm{Re}\,\sigma>0$) in the discrete (●) system, even though all continuum (—) modes remain stable. For this smaller valuer of τ the other six continuum modes have $\mathrm{Re}\,\sigma \approx -5$, and so are off the bottom of the figure.

both discrete and continuum systems as functions of $k_x=k_y$ (recall that instability only occurs for $k_xk_y\neq 0$) for the parameters $\tau=1,P=0,Q=-\frac{1}{3}\rho$ (Fig. 3) and $Q=+\frac{1}{3}\rho$ (Fig. 4). Three eigenvalues vanish in the long wave ($\mathbf{k}\to\mathbf{0}$) limit, for both the discrete and the continuous systems, corresponding to conservation of density and the two components of momentum under collisions. The remaining six eigenvalues emerge from $-1/\tau$ in the continuous system (49), and from $\log|(1-2\tau)/(1+2\tau)|$ in the discrete system (48). Instability, meaning an eigenvalue with positive real part, only occurs for $dQ/d\rho>0$, as predicted by the analysis above, and shown in Fig. 4. For $dQ/d\rho<0$, which includes the Hermite expansion with $dQ/d\rho\approx-\frac{1}{3}$, only stable oscillations occur (Fig. 3), again in agreement with the above analysis in Sec. VII.

However, lattice Boltzmann schemes are typically used in parameter regimes where $\tau<\frac{1}{2}$ in lattice units. They attain low net diffusivities, or high Reynolds numbers, through an almost exact cancellation between negative diffusion, from the $O(\Delta x)$ spatial truncation error, and positive diffusion from collisions. In this instance, instability does arise for $dQ/d\rho<0$ as shown in Fig. 5, but only for wave vectors $\mathbf{k}$ large enough that the behavior of the discrete system is no longer close to the continuum system. Thus the continuum analysis of Sec. VII serves only to identify a mechanism, and the criterion $Q=0$ to eliminate the instability. We believe this approach is more illuminating than a computational search for unstable eigenvalues in a five or larger dimensional parameter space.

IX. CONCLUSION

The most common two-dimensional lattice Boltzmann scheme uses nine particle speeds arranged on a square lattice as in Fig. 2. Simulating the viscous compressible Navier-Stokes, shallow water, or general barotropic fluid, equations impose only eight constraints on the equilibrium distribution functions. In this paper we have explored an instability associated with the remaining single degree of freedom, identified with a nonhydrodynamic ghost mode. Eliminating this instability provides one more constraint, $Q=0$ in Eq. (43), and so serves to determine the unique set of equilibria that yield a usable computational scheme. With respect to understanding the instability mechanism, and a criterion for removing it, the approximate analytical treatment in Sec. VII is more useful than the numerical solution of eigenvalue problems in Sec. VIII.

The equilibrium distribution functions given by a truncated expansion in tensor Hermite polynomials [11], as advocated by the *a priori* approach [9,10,17,33], coincide with those determined by the ghost mode stability condition for the isothermal Navier-Stokes equations. For general equations of state the Hermite polynomial expansion leads to unstable schemes, and must be modified in the fashion described above. We are unable to offer an explanation of why the Hermite expansion happens to work for the isothermal Navier-Stokes equations.

This scheme may be used for nonideal barotropic equations of state other than the shallow water equations, provided the pressure $P(\rho)$ appears in the Hermite expansion as above, and the function $N^{(0)}(\rho)$ is chosen to eliminate the density gradient term in Eq. (42). The Enskog equation, an extension of the Boltzman equation to dense (nondilute) gases studied recently by Luo [17], yields a barotropic equation of state $P=\theta\rho(1+bg\rho)$ for small density fluctuations, where the virial coefficients b and g have been calculated as perturbation series in ρ [26,28]. Our approach offers an alternative lattice Boltzmann formulation to Luo's [17] for gases described by the Enskog equation, and one that does not require a density gradient computed by finite difference approximation, which in turn complicates the treatment of boundaries. On the other hand, our approach gives a viscous stress that is not quite Newtonian, as calculated in Appendix A, but the deviation will be small for nearly ideal gases.

Returning to geophysical applications, we have used this scheme to simulate Bühler's modified shallow water equations [37] with $P=-1/(2\rho^2)$. This equation of state has the property of allowing steadily propagating one-dimensional simple waves with smooth profiles in the absence of viscosity, while being equivalent to the conventional shallow water equations for small amplitude (linear) waves. This modification suppresses the formation of shocks, that are often an unnecessary nuisance when the shallow water equations are used as a prototype for the meteorological primitive equations, say, that do not form shocks.

Other recent work has tried to extend the lattice Boltzmann approach to finite Mach number and nonisothermal flows with a correct internal energy equation. Different approaches using differing equilibria and numbers of particle speeds have met with varying degrees of success and stability at finite Mach numbers [19–21]. Again, the constraints needed to derive the viscous, thermally conducting Navier-

Stokes-Fourier equations do not determine a unique set of equilibria [19].

Finally, it is interesting to note (see Appendix B for details) that the shallow water equations provide a counterexample to the arguments in Ref. [38] for the stability of lattice Boltzmann schemes where separate particle distribution functions are restricted to be either always positive or always negative, and for the instability of schemes in which distribution functions change sign. The equilibria necessary for a stable shallow water scheme, those that eliminate the ghost mode instability, turn out to be precisely those that most encourage distribution functions to change sign.

ACKNOWLEDGMENTS

Rick Salmon kindly supplied copies of his papers [2,3], and drew the author's attention to Ref. [23]. Financial support from St. John's College, Cambridge, UK, is gratefully acknowledged.

APPENDIX A: THE DISSIPATIVE STRESS

Equation (14) expresses the dissipative stress $\mathbf{\Pi}^{(1)}$ that appeared in Sec. IV in terms of $\Sigma_i \boldsymbol{\xi}_i \boldsymbol{\xi}_i \boldsymbol{\xi}_i f_i^{(0)}$, and the known quantities $\partial_{t_0}\rho$ and $\partial_{t_0}(\rho\mathbf{u})$. In this appendix we compute $\mathbf{\Pi}^{(1)}$ for a general barotropic equation of state $P(\rho)$. In continuum kinetic theory the third tensor Hermite moment is independent of the lower moments [11,27], but in the two-dimensional, nine speed discrete system $\Sigma_i \boldsymbol{\xi}_i \boldsymbol{\xi}_i \boldsymbol{\xi}_i f_i^{(0)}$ is determined completely by the vectors $\mathbf{J}^{(0)}$ and $\rho\mathbf{u}$ via Eqs. (39a,b). For $f_i^{(0)}$ given by Eq. (38) with $\mathbf{J}^{(0)}=0$, and $N^{(0)}$ arbitrary

$$\sum_{i=0}^{8} \xi_{i\alpha}\xi_{i\beta}\xi_{i\gamma}f_i^{(0)} = \theta\rho(u_\alpha\delta_{\beta\gamma}+u_\beta\delta_{\gamma\alpha}+u_\gamma\delta_{\alpha\beta}). \quad \text{(A1)}$$

We follow Ref. [1] in using Greek indices for vector components, as Roman indices have been used to label the discrete velocity vectors $\boldsymbol{\xi}_i$. Using Eq. (15), the other term $\partial_{t_0}\mathbf{\Pi}^{(0)}$ contributing to the dissipative stress is

$$\begin{aligned}\partial_{t_0}\Pi^{(0)}_{\alpha\beta} =& -\left(\frac{dP}{d\rho}\delta_{\alpha\beta}-u_\alpha u_\beta\right)\nabla\cdot(\rho\mathbf{u}) - u_\alpha\left(\frac{dP}{d\rho}\frac{\partial\rho}{\partial x_\beta}\right.\\ &\left.+\frac{\partial}{\partial\gamma}(\rho u_\beta u_\gamma)\right) - u_\beta\left(\frac{dP}{d\rho}\frac{\partial\rho}{\partial x_\alpha}+\frac{\partial}{\partial\gamma}(\rho u_\alpha u_\gamma)\right),\\ =& -\frac{dP}{d\rho}\left(\delta_{\alpha\beta}\nabla\cdot(\rho\mathbf{u})+u_\alpha\frac{\partial\rho}{\partial x_\beta}+u_\beta\frac{\partial\rho}{\partial x_\alpha}\right)\\ &-\frac{\partial}{\partial\gamma}(\rho u_\alpha u_\beta u_\gamma). \end{aligned} \quad \text{(A2)}$$

The total dissipative stress is therefore

$$\begin{aligned}\Pi^{(1)}_{\alpha\beta} =& -\tau\left[\theta\rho\left(\frac{\partial u_\alpha}{\partial x_\beta}+\frac{\partial u_\beta}{\partial x_\alpha}\right)+\left(\theta-\frac{dP}{d\rho}\right)\left(\delta_{\alpha\beta}\nabla\cdot(\rho\mathbf{u})\right.\right.\\ &\left.\left.+u_\alpha\frac{\partial\rho}{\partial x_\beta}+u_\beta\frac{\partial\rho}{\partial x_\alpha}\right)-\frac{\partial}{\partial\gamma}(\rho u_\alpha u_\beta u_\gamma)\right], \end{aligned} \quad \text{(A3)}$$

where the first term is the usual Navier-Stokes viscous stress, with shear viscosity $\mu=\tau\theta\rho$, and bulk viscosity $\frac{2}{3}\mu$ [22,35]. For nonzero $\mathbf{J}^{(0)}$, Eq. (A3) becomes

$$\mathbf{\Pi}^{(1)} = \mathbf{\Pi}^{(1)}\Big|_{\mathbf{J}^{(0)}=\mathbf{0}} - \frac{\tau}{6}\begin{pmatrix}\partial_y J_y^{(0)} & \partial_x J_y^{(0)}+\partial_y J_x^{(0)}\\ \partial_x J_y^{(0)}+\partial_y J_x^{(0)} & \partial_x J_x^{(0)}\end{pmatrix} \quad \text{(A4)}$$

using Eqs. (40a,b). Thus $\mathbf{J}^{(0)}$ must vanish to recover the correct continuum behavior, as asserted in Sec. VI, but $N^{(0)}$ remains undetermined.

The final term $\nabla\cdot(\rho\mathbf{uuu})$ in Eq. (A3) is $O(\mathrm{Ma}^3)$ in the usual lattice Boltzmann scalings, so it is usually negligible in comparison with the other terms. It may be eliminated by modifying the equilibrium distribution $f_i^{(0)}$ to add a term $\rho u_\alpha u_\beta u_\gamma$ to Eq. (A1), but this requires a larger lattice with 13 or more particle speeds instead of nine [19–21].

The second term in Eq. (A3), proportional to $(\theta - dP/d\rho)$, vanishes for the isothermal Navier-Stokes case, where $P=\theta\rho$, owing to an exact cancellation of the density gradient between the two terms in Eq. (14). Thus the lattice Boltzmann equation for the isothermal Navier-Stokes correctly simulates a Newtonian fluid, with a viscous stress proportional to the symmetric part of the *velocity* gradient [35]. For the shallow water equations, $P=\frac{1}{2}g\rho^2$, this lattice Boltzmann treatment yields a dissipative stress involving the *momentum* gradient, plus corrections of $O(\mathrm{Ma}^2/\mathrm{Fr}^2)$. This distinction is particularly significant for the shallow water equations, where density gradients may be $O(1)$, rather than only $O(\mathrm{Ma}^2)$ in the weakly compressible Navier-Stokes equations. The dissipation takes the form [2]

$$\nabla\cdot\mathbf{\Pi}^{(1)} = -\tau\theta[\nabla^2(\rho\mathbf{u})+2\nabla\nabla\cdot(\rho\mathbf{u})+O(\mathrm{Ma}^2/\mathrm{Fr}^2)], \quad \text{(A5)}$$

where the Froude number $\mathrm{Fr}=u/\sqrt{g\rho}$ is the ratio of the fluid speed to the surface gravity wave speed. The $O(\mathrm{Ma}^2/\mathrm{Fr}^2)$ term is due to the time derivative $\partial_{t_0}\mathbf{\Pi}^{(0)}$, and may be made arbitrarily smaller than the other two terms by taking the Mach number to be sufficiently small, equivalent to taking sufficiently small time steps. This form of dissipation is somewhat unsatisfactory in principle because it is not Galilean invariant, and the resulting "dissipation" of the total energy density $\frac{1}{2}\rho|\mathbf{u}|^2+\frac{1}{2}g\rho^2$ is, in fact, not sign definite. However, by being the divergence of a symmetric tensor this form of dissipation is at least momentum and angular momentum conserving, and so is preferable to just $\nabla^2(\rho\mathbf{u})$ as used in some previous ocean models, according to the criteria of Shchepetkin and O'Brien [23]. In particular, Shchepetkin and O'Brien [23] found that asymmetric viscous stress 'tensors could generate spurious vorticity, and by amounts that did not vanish with increasing spatial resolution.

A Newtonian viscous stress could be obtained by modifying the equilibria $f_i^{(0)}$ to make the third moment in Eq. (A1) equal to $P(\rho)(u_\alpha\delta_{\beta\gamma}+u_\beta\delta_{\gamma\alpha}+u_\gamma\delta_{\alpha\beta})$, equivalent to replacing what was the isothermal pressure $\rho\theta$ by the correct pressure $P(\rho)$. This change would require 13 or more particle speeds instead of nine speeds [20]. Equation (A3) would then give a Newtonian viscous stress with dynamic viscosity $\mu=P(\rho)\tau$. The collision rate τ may be made a function of ρ, for example, $\tau\propto 1/P(\rho)$ gives a spatially uniform dynamic viscosity [33]. For shallow water, $\tau\propto 1/\rho$ gives $\mu\propto\rho$ as recommended by Refs. [23,24] for a sign definite energy dissipation.

APPENDIX B: DISTRIBUTION FUNCTION SIGNS

A possible alternative argument for choosing the equilibria Eq. (27) in preference to Eq. (23) is that all nine $f_i^{(0)}$ in Eq. (27) are positive in a rest state with $\mathbf{u}=\mathbf{0}$. If we consider the more general form

$$f_i^{(0)}=w_i\left(\rho+\frac{1}{\theta}(\rho\mathbf{u})\cdot\boldsymbol{\xi}_i+\frac{1}{2\theta^2}[(P(\rho)-\theta\rho)\mathsf{I}+\rho\mathbf{uu}]:(\boldsymbol{\xi}_i\boldsymbol{\xi}_i-\theta\mathsf{I})\right)+w_ig_i\lambda\left(\frac{1}{4}\rho-\frac{3}{8}g\rho^2\right) \tag{B1}$$

with an adjustable parameter λ, the equilibrium distributions at rest are

$$f_0^{(0)}=\frac{8+\lambda}{9}\rho-\frac{4+\lambda}{6}g\rho^2,\quad f_{1234}^{(0)}=\frac{1-\lambda}{18}\rho+\frac{1+\lambda}{12}g\rho^2,$$
$$f_{5678}^{(0)}=\frac{\lambda-1}{36}\rho+\frac{2-\lambda}{24}g\rho^2. \tag{B2}$$

Since $g\rho=O(|\mathbf{u}|^2)=O(\mathrm{Ma}^2)\ll 1$ in our scalings, $\lambda=1$ is the unique choice that makes all the $f_i^{(0)}$ positive in the small Mach number limit. This has been presumed to be beneficial for stability [38]. However, for $\lambda=1$ and $i\neq 0$ the $f_i^{(0)}$ take the form $f_i^{(0)}=3w_i\,\boldsymbol{\xi}_i\cdot\mathbf{u}+O(\mathrm{Ma}^2)$. The first term is typically the larger in magnitude, being $O(\mathrm{Ma})$ rather than $O(\mathrm{Ma}^2)$, and is equally likely to be either positive or negative. The equilibria in Eqs. (26a,b) are thus of indefinite sign, except for rest states with $\mathbf{u}=\mathbf{0}$.

[1] S. Chen, and G.D. Doolen, Annu. Rev. Fluid Mech. **30**, 329 (1998).

[2] R. Salmon, J. Mar. Res. **57**, 503 (1999).

[3] R. Salmon, J. Mar. Res. **57**, 847 (1999).

[4] R. Salmon, *Lectures on Geophysical Fluid Dynamics* (Oxford University Press, Oxford, 1998).

[5] J. Pedlosky, *Geophysical Fluid Dynamics*, 2nd ed. (Springer, New York, 1987).

[6] U. Frisch, B. Hasslacher, and Y. Pomeau, Phys. Rev. Lett. **56**, 1505 (1986).

[7] G.R. McNamara and G. Zanetti, Phys. Rev. Lett. **61**, 2332 (1988).

[8] Y.H. Qian, D. d'Humières, and P. Lallemand, Europhys. Lett. **17**, 479 (1992).

[9] X. He and L.-S. Luo, Phys. Rev. E **56**, 6811 (1997).

[10] X. Shan, and X. He, Phys. Rev. Lett. **80**, 65 (1998), comp-gas/9712001.

[11] H. Grad, Commun. Pure Appl. Math. **2**, 325 (1949).

[12] J.D. Sterling and S. Chen, J. Comput. Phys. **123**, 196 (1996) (e-print comp-gas/9306001).

[13] P. Lallemand, and L.-S. Luo, Phys. Rev. E **61**, 6546 (2000); ICASE Report No. TR-2000-17, Institute for Computer Applications in Science and Engineering, NASA Langley Research Center.

[14] R. Benzi, S. Succi, and M. Vergassola, Europhys. Lett. **13**, 727 (1990).

[15] R. Benzi, S. Succi, and M. Vergassola, Phys. Rep. **222**, 145 (1992).

[16] D. d'Humières, in *Rarefied Gas Dynamics: Theory and Simulations, Prog. Astronaut. Aeronaut*, edited by B.D. Shizgal and D.P. Weaver (AIAA, Washington, DC, 1992), Vol. 159, pp. 450–458.

[17] L.-S. Luo, Phys. Rev. E **62**, 4982 (2000); ICASE Report No. TR-2001-8, Institute for Computer Applications in Science and Engineering, NASA Langley Research Center.

[18] P.J. Dellar, J. Comput. Phys. (to be published).

[19] Y. Chen, H. Ohashi, and M. Akiyama, Phys. Rev. E **50**, 2776 (1994).

[20] J.R. Weimar and J.P. Boon, Physica A **224**, 207 (1996).

[21] Y.-H. Qian and Y. Zhou, Europhys. Lett. **42**, 359 (1998); ICASE Report No. TR-98-38, Institute for Computer Applications in Science and Engineering, NASA Langley Research Center.

[22] L. D. Landau and E. M. Lifshitz, *Fluid Mechanics*, 2nd ed. (Pergamon, Oxford, 1987).

[23] A.F. Shchepetkin and J.J. O'Brien, Mon. Weather Rev. **124**, 1285 (1996).

[24] C. Schär and R.B. Smith, J. Atmos. Sci. **50**, 1373 (1993).

[25] K. Huang, *Statistical Mechanics*, 2nd ed. (Wiley, New York, 1987).

[26] G.E. Uhlenbeck and G.W. Ford, *Lectures in Statistical Mechanics, Lectures in Applied Mathematics* (American Mathematical Society, Providence, RI, 1963), Vol. 1.

[27] H. Grad, in *Thermodynamik der Gase, Handbuch der Physik*, edited by S. Flügge (Springer, Berlin, 1958), Vol. 12, pp. 205–294.

[28] S. Chapman, and T.G. Cowling, *The Mathematical Theory of Non-Uniform Gases*, 3rd ed. (Cambridge University Press, Cambridge, 1991).

[29] C. Cercignani, *The Boltzmann Equation and its Applications* (Springer, New York, 1988).

[30] P.L. Bhatnagar, E.P. Gross, and M. Krook, Phys. Rev. **94**, 511 (1954).
[31] K. Xu, in *29th Computational Fluid Dynamics*, lecture series 1998-03 (von Karman Institute, Belgium, 1998), available from http://www.math.ust.hk/~makxu/PAPER/VKI_LECTURE98.ps.
[32] K. Xu, Int. J. Mod. Phys. C **10**, 505 (1999).
[33] P.J. Dellar, Phys. Rev. E (to be published).
[34] P.J. Davis and P. Rabinowitz, *Methods for Numerical Integration*, 2nd ed. (Academic, New York, 1984).
[35] P.J. Dellar, Phys. Rev. E **64**, 031203 (2001).
[36] E. Anderson, *et al.*, *LAPACK Users' Guide*, 3rd ed. (SIAM, Philadelphia, 1999).
[37] O. Bühler, J. Atmos. Sci. **55**, 2884 (1998).
[38] M. De Cicco, S. Succi, and G. Bella, SIAM J. Sci. Comput. **21**, 366 (1999).